Title: Fabrication of New Photoactuators: Macroscopic Photomechanical Responses of Metal-Organic Frameworks to Irradiation by UV Light

Authors: Yi-Xiang Shi; Wen-Hua Zhang, Ph.D; Brendan F. Abrahams, Ph.D; Pierre Braunstein, Ph.D; Jian-Ping Lang, Prof. Dr.

To be cited as: 10.1002/anie.201903757

Link to VoR: https://doi.org/10.1002/anie.201903757

Fabrication of New Photoactuators: Macroscopic Photomechanical Responses of Metal-Organic Frameworks to Irradiation by UV Light

Yi-Xiang Shi, Wen-Hua Zhang, Brendan F. Abrahams, Pierre Braunstein, and Jian-Ping Lang*

Abstract: Photoactuators capable of converting light energy into mechanical work at the macroscopic level are of considerable interest in a wide variety of soft robotic systems. Although stimulus-responsive materials, which result in geometric deformations, have been developed it is only recently that photo-triggered actuators, which allow self-propelled motion, have been included in metal-organic frameworks (MOFs). Herein we describe the incorporation of photoreactive olefinic species into a MOF, [Zn(bdc)(3-F-spy)] (**1**). Single crystals of **1** are shown to undergo three types of photomechanical macroscopic deformation upon illumination by UV light. In an effort to demonstrate the practical potential of this system, the inclusion of **1** in a PVA (polyvinyl alcohol) composite membrane, by exploiting hydrogen-bonding interactions, is presented. Using this novel composite membrane the amplification of mechanical stress to achieve macroscopic actuation behavior is demonstrated. Our results pave the way for the generation of MOF-based soft photoactuators that produce clearly defined mechanical responses upon irradiation with light. Such systems are anticipated to have considerable potential in photomechanical energy harvesting and conversion systems.

Actuation materials that effectively convert external controllable stimuli to mechanical energy have recently attracted attention in the fields of soft robotics,[1] biomedicine,[2] biomimetic systems[3] and molecular machines[4] with synthetic materials having the potential to undergo intended deformations involving twisting, bending, swimming, and elongation/contraction.[5] Various types of smart actuation driven by external physical or chemical stimuli (e.g. heat,[6] electricity,[7] magnetism,[8] humidity[9] or light[10]) have been extensively investigated and developed. The design and fabrication of a smart actuation that can achieve multiple desired deformations and perform target functions represent essential prerequisites.[4a,11] Accordingly, the manipulation and deformation of actuation associated with rapid and precise response is of great relevance to both fundamental research and practical applications toward the prompt and effective conversion of external stimuli to mechanical movement.[12]

As a branch of stimuli-responsive actuation, photoactuators is particularly attractive for energy conversion as they can be triggered externally in a non-invasive, non-contact manner, and as such they are particularly attractive for practical applications.[13] Recent progress in the field of photoactuation has focused on deformation by photochemical reactions and photothermal effects.[10a,14] The actuation mechanism for photoinduced motion is well established for photo-responsive molecules including diarylethene,[15] anthracene,[16] Schiff bases[17] and azobenzene[18] which undergo reversible shape deformations upon photoirradiation. As a consequence, actuators have been designed and manufactured by incorporating photo-responsive molecules into liquid crystalline polymer networks, hydrogels or molecular crystals. Within these matrices the photoresponsive molecules serve as molecular photo-switches that are able to produce rapid and reversible macroscopic motion upon irradiation.[19] Despite these responses upon exposure to light, the anisotropy of macroscopic mechanical movement is strongly associated with the degree of crystallinity, free volume, and molecular orientation of the photoresponsive molecule.[20] Thus, the design and fabrication of anisotropic photoactuation systems by a bottom-up approach leading to a hierarchical structure that can convert photonic energy into mechanical energy at the macroscopic scale still remains a formidable challenge.[5b,21]

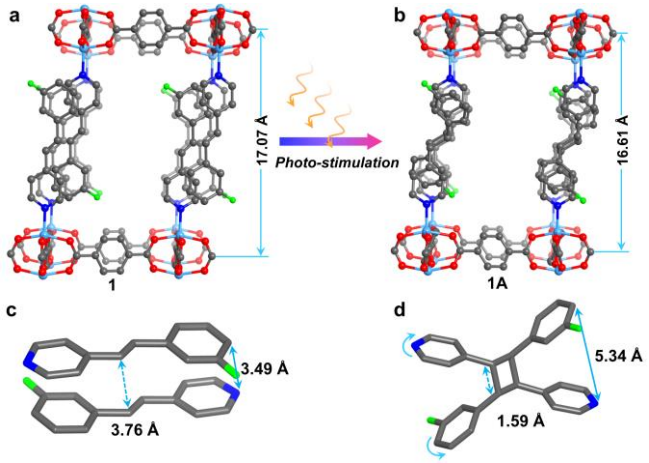

Figure 1. Structural representation of photo-induced lattice contraction. a, b) View along the *b* axis of **1** and **1A**. (c) View of the head-to-tail molecular packing of photoreactive ligands in **1**. d) The structure of photodimerization ligand in **1A**. Sky blue arrows represent significant separations in **1** and **1A**.

[*] Y. X. Shi, Prof. W. H. Zhang, Prof. J. P. Lang
College of Chemistry, Chemical Engineering and Materials Science, Soochow University, No.199 RenAi Road, Suzhou 215123, Jiangsu (P. R. China)
E-mail: jplang@suda.edu.cn
Prof. J. P. Lang
State Key Laboratory of Organometallic Chemistry, Shanghai Institute of Organic Chemistry, Chinese Academy of Sciences, Shanghai 200032 (P. R. China)
Prof. B. F. Abrahams
School of Chemistry, University of Melbourne, Victoria 3010 (Australia)
Prof. P. Braunstein
Institut de Chimie (UMR 7177 CNRS), Université de Strasbourg, 4 rue Blaise Pascal-CS 90032, 67081 Strasbourg (France)

Supporting information for this article is given via a link at the end of the document.

Metal-organic frameworks (MOFs) constructed from metal-containing secondary building units and organic linkers have emerged as a class of hierarchically ordered porous crystalline materials with widespread applications in the fields of gas storage and separation,[22] chemical sensing,[23] drug delivery,[24] heterogeneous catalysis[25] and solar energy harvesting[26] owing much to their thermal and chemical stability, functional diversity and structural tenability. The incorporation of photoactive units into a MOF structure offers the prospect of producing a crystalline material in which photoresponsive molecules are not only arranged in a periodic manner but also aligned in a way that will deliver macroscopic movement upon irradiation.[27] Herein we report a self-assembly strategy for the fabrication of hierarchical photoactuator system in which photoresponsive units are incorporated into a MOF structure. Irradiation of [Zn(bdc)(3-F-spy)] (**1**, 3-F-spy = 4-(3-fluorostyryl)pyridine; H_2bdc = 1,4-benzenedicaboxylic acid) with 365 nm light results in [2+2] photodimerization reactions that in turn lead to geometrical changes to individual crystals. Photomechanical twisting and bending have been investigated in slender and rod-like crystals. A detailed understanding of the photomechanical actuation mechanism of single crystals of **1** has been obtained. Of particular importance is the fabrication of a photoactuation system involving a composite membrane formed from the combination of PVA and **1**. The membrane exhibits a clear photomechanical response to irradiation with UV light. To the best of our knowledge, the findings in the present work demonstrate, for the first time, a photoactuation system based on photoresponsive MOFs.

Colorless block crystals of **1** were derived from the solvothermal reactions of $ZnSO_4{\cdot}7H_2O$, H_2bdc and 3-F-spy in DMF-H_2O mixed solvents at 145 °C for 12 h. The phase purity of bulk crystalline material was well confirmed by comparison of the experimental powder X-ray diffraction pattern with the simulated powder X-ray diffraction pattern derived from the single crystal data (Figure S1). Single crystal X-ray diffraction (SCXRD) analysis revealed that **1** crystallized in the monoclinic space group *C*2/*c*. The crystallographic asymmetric unit of **1** is comprised of one Zn(II) ion, two distinct half bdc^{2-} linkers and one 3-F-spy ligand (Figure S2). The combination of Zn(II) centres and bdc^{2-} anions yields a polymeric structure in which pairs of Zn(II) centres are linked by four carboxylate groups to form a $[Zn_2(OOC)_4]$ paddle-wheel type unit that serves as a 4-connecting unit in a 2D square grid-type polymeric structure. The coordination environment of each Zn centre is completed by the pyridyl nitrogen atom of a 3-F-spy ligand to produce a slightly distorted square pyramidal coordination geometry with the four carboxylate oxygen atoms forming the square base and the nitrogen donor of the 3-F-spy ligand occupying the apex of the pyramid. With each of the Zn centres of the paddle-wheel unit coordinated by a 3-F-spy ligand, the structure consists of a 2-D network with the terminal 3-F-spy ligand extending above and below the sheet (Figures S3-S5). Each coordinated 3-F-spy ligand passes through a $(Zn_2)_4(bdc)_4$ rhombic-shaped hole of an adjacent parallel sheet where it associates, in a head-tail arrangement, with a 3-F-spy ligand originating from the opposite direction. Intermolecular π–π interactions exist between the pair of 3-F-spy ligands located within the rhombic-shaped hole of an intermediate $Zn_2(bdc)_2$ sheet (Figures S6 and S7). The alignment of the olefinic bonds, which are *ca.* 3.76 Å apart, places them in an arrangement suitable for photodimerisation to occur (Figure 1a, c).[28] Thermal gravimetric analysis (TGA) of **1** indicates no weight loss up to 300 °C under N_2 after which, thermal decomposition occurs (Figure S8a). In addition, no appreciable N_2 adsorption could be observed with a Brunauer–Emmett–Teller (BET) specific surface area of 6.4 $m^2\ g^{-1}$, which is consistent with the calculated results of the total accessible volumes by PLATON software (about 7.8%) (Figure S8b).

As part of an evaluation of the photoactivity of **1** the ultraviolet–visible (UV-vis) absorption spectra of both 3-F-spy and **1** were recorded. The UV-vis absorption spectra of 3-F-spy and **1** indicated a broad absorption band in the range 200−425 nm (Figure S9). A significant enhancement of the absorbance of **1** was observed compared to the free ligand (3-F-spy) is attributed to either metal to ligand or ligand to ligand charge transfer (LLCT/MLCT). The broad absorption band of **1** containing photoreactive units encouraged us to investigate its photo-responsive behavior. Upon irradiation at 365 nm wavelength light equipped with internal heat filter at room temperature on its (0-10) plane for *ca.* **1** min, the aligned 3-F-spy ligands undergo photodimerisation to form a *rctt*-1,3-bis(4-pyridyl)-2,4-bis(3-fluorophenyl)cyclobutane (*rctt*-ppcb) which provides a covalent link between Zn_2bdc_2 sheets. Each *rctt*-ppcb ligand passes through a $(Zn_2)_4bdc_4$ square hole and thus the 2D structure of **1** is transformed into two crystallographically equivalent interpenetrating frameworks of composition $[Zn(bdc)(rctt\text{-ppcb})_{0.5}]$ (**1A**) in a single-crystal to single-crystal (SCSC) transformation (Figure 1b, d, Figure S10 and Figure S11). The transformation of **1** to 1A results in a contraction of the unit cell volume by 6.1% (3908.3 $Å^3$ to 3669.7 $Å^3$). In regards to the cell axes, the most significant decrease is in the *a* axis (6.67%) whilst the *b* axis shows only a modest decrease (0.87%). A slight increase is noted in the *c* axis from 18.73 to 18.87 Å. This is in contrast with the anti-parallel arrangement of the unreacted ligands depicted in Figure 1c. The dimerisation of the 3-F-spy ligands is accompanied by geometrical changes in the $Zn_2(bdc)_2$ sheets. Firstly, the aromatic rings which adopted a conformation in which they were almost normal to the mean plane of the $Zn_2(bdc)_2$ network in **1** are significantly inclined in **1A** (Figure S12). In addition, the $Zn_2(bdc)_2$ network undergoes a shear distortion with Zn···Zn···Zn angles within a rhombic cavity changing from 75.41 and 104.59° in **1** to 71.3 and 108.62° in **1A**.

The type of anisotropic lattice contraction demonstrated in the photo-induced transformation of **1** to **1A** has been identified in actuators that exhibit mechanical responses to external stimuli.[29] In order to investigate whether the lattice contraction that occurs when **1** is transformed to **1A** is able to produce a measurable macroscopic change, a long single crystal of **1** (0.11 × 0.13 × 2.62 mm) was irradiated UV-light and the physical appearance of the crystal was monitored. The changes accompanying the exposure to UV light are depicted in Figure 2a and in Movie S1. Initially, the crystal bent towards the incident 365 nm light, reaching a bending angle of approximately 80° within 1 second. The crystal then rapidly twisted into the right-hand helical shape within 15 seconds as the photoreaction involving the dimerisation of coordinated 3-F-spy ligands transforms the 2D structure of **1** to the interpenetrating 3D structure of **1A**. Noticeably, the crystal retained its helical

morphology when the light is switched off (Figure S14). Further irradiation experiments revealed that the generation of the right-handed helix morphology was independent of the direction of the light source. The rapid and substantial change in the crystal shape (80° s^{-1}) is attributed to the lattice contraction of 6.1% upon irradiation and is in contrast to photoresponsive shape-memory polymer-based actuators[30] that exhibit a slower mechanical response upon irradiation.

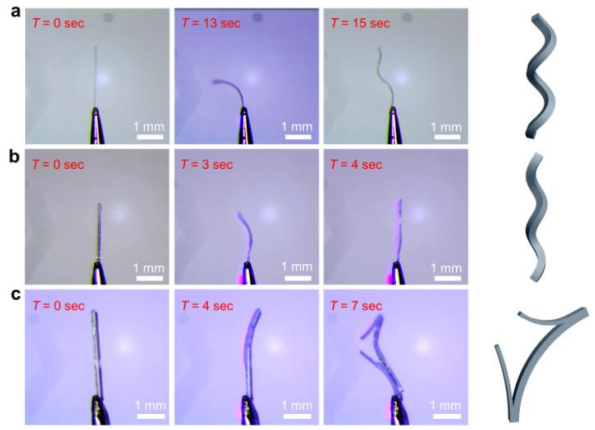

Figure 2. Optical microscope images of photomechanical deformations of crystal **1** induced by UV irradiation light. a–c) The photo-induced helix, twisting and splitting morphology transformation of single crystal **1** with difference size. The crystal was fixed to a pin sample holder and UV irradiation was conducted from the left side on the image.

Previous work described in the literature indicates that the magnitude of mechanical deformation of a photo-sensitive crystal is sensitive to the dimensions of the crystal.[31] To ascertain whether the extent and type of mechanical distortion is affected by the crystal dimensions in the case of **1**, an investigation was undertaken whereby different sized crystals were irradiated with UV light. As crystal of dimensions 0.18 × 0.21 × 2.29 mm, which is significantly thicker than the crystal depicted in Figure 2a, was found to bend towards the incident light source before undergoing a transformation to a helically twisted needle (Figure 2b, Figure S15 and Movie S2). When a slightly thicker and longer crystal (0.26 × 0.21 × 3.25 mm) was used, the crystal gradually bends away from the incident light. With prolonged irradiation a sudden release of strain energy resulted in the crystal splitting into several pieces as depicted in Figure 2c, Figure S16 and Movie S3. It has been proposed that these types of transformations result from the alleviation of long-order interfacial strain in crystals arising from changes in molecular structure that occur upon irradiation.[32] The results imply that the observed transformation is a consequence of a delicate balance of factors including crystal dimensions, tensile stress and the exposure time to the incident light source.

To elucidate the photomechanical actuation mechanism, a high quality, single crystal of **1** was exposed to 365 nm light for 15 seconds. This irradiation leads to the generation of **1B** which may be considered to be a crystal representing an intermediate form of **1** and **1A** i.e. one in which only a proportion of the 3-F-spy ligands has undergone photodimerisation. Single crystal X-ray analysis reveals that **1B** adopts the same monoclinic space group, *C*2/*c,* as both **1** and **1A** (Table S3). The crystal structure refinement reveals the presence of both the unreacted and dimerised 3-F-spy ligands which appear as overlapping molecules each with partial occupancies. Refinement of site occupancies indicate that approximately 23% of the ligands have undergone dimerisation (Figure 3). The partial conversion of **1** to **1A** results in a contraction mainly along the *a* axis (1.14%) which is accompanied by a unit cell volume contraction of about 1.26% from 3908.3 $Å^3$ to 3859.1 $Å^3$ (Figure 3b). It is proposed that the partial photoconversion of the crystal, as indicated by the structure determination of **1B**, is responsible for the introduction of forces across interfacial regions within the crystal, leading to the observed macroscopic deformations of the type depicted in Figure 2.

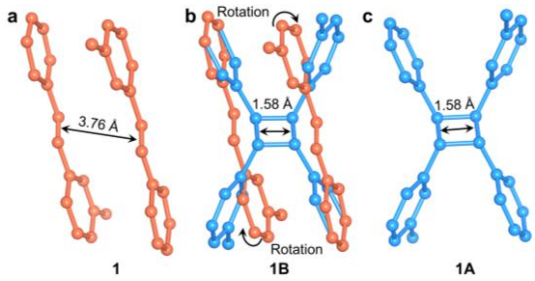

Figure 3. Light-induced [2+2] cycloaddition reaction occurring within a single crystal of **1**. a–c) Portions of the structures of **1**, **1B** and **1A** with indicated C···C distance. Sky blue and orange represent the structure of 3-F-spy and *rctt*-ppcb, respectively. For clarity, hydrogen atoms have been omitted.

In addition to single crystal data, *in situ* PXRD was employed to confirm the transformation of 3-F-spy to *rctt*-ppcb upon exposure to light. As shown in Figure 4, the sharp pristine (022), (40-2), (22-1) and (221) peaks at 2θ = 10.7°, 16.5°, 18.0° and 20.6° diminish and almost completely disappear during irradiation over a period 15 seconds, while the (200), (202) and (20-2) peaks gradually split into two new peaks. However, two distinct new peaks appeared at 2θ = 19.5° and 21.4° over the irradiation period (Figure S17). ^{1}H or ^{13}C NMR a sample of **1** after exposure for more than 40 seconds indicate complete photochemical conversion (Figures S18-S21).

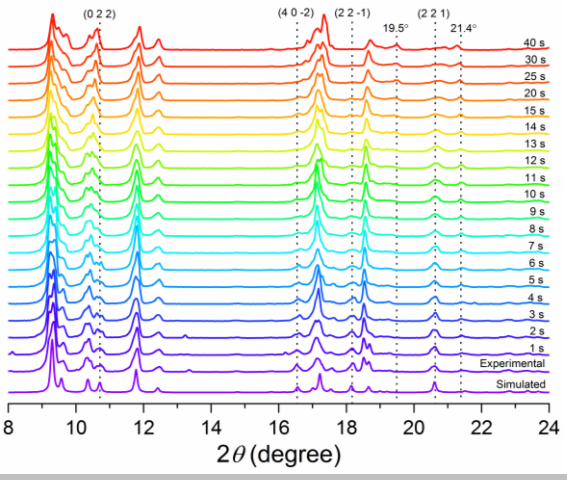

Figure 4. *In situ* PXRD spectra of crystalline **1** as a function of irradiation time at room temperature. The as-prepared **1** was converted to **1A** phase by irradiation for 20 seconds.

Generally, inorganic and crystalline materials are brittle in comparison with soft materials[33] and thus in isolation they are unlikely to fulfill a useful technological role in which predictable macroscopic responses to irradiation are required. We describe here a macroscopic photoactuation device in which the photoactive MOF is combined with polyvinyl alcohol (PVA) to form a composite membrane. It is known that, the orientation and distribution of photo-responsive moieties in composite membranes can play a critical role in modulating the photomechanical actuation. It is proposed that the hydrophilic PVA polymer, with abundant OH groups, can interact with F atoms of the MOF through the formation of O–H···F hydrogen bonds.[34a] The fabrication process for the photoactuator is presented schematically in Figure 5. The homogeneous **1**-PVA composite membrane with uniform thickness (~3 μm) was successfully constructed and characterized by scanning electron microscopy (SEM) image and PXRD patterns (Figures 5b-d). In the IR of **1**-PVA, the O–H stretching vibration was shifted to the lower wavenumber at 3250 cm^{-1} compared with that of pure PVA (3404 cm^{-1}), suggesting the formation of stronger O–H···F bonding interactions[34b] between the OH groups of PVA and the F atoms of 3-F-spy ligands in **1** (Figure S22). The SEM image with EDX of **1**-PVA composite membrane indicated the formation of a homogeneous composite membrane (Figures 5c, S23 and S24). The PXRD patterns of the **1**-PVA membrane matched the combined patterns of PVA and **1** (Figure 5d).

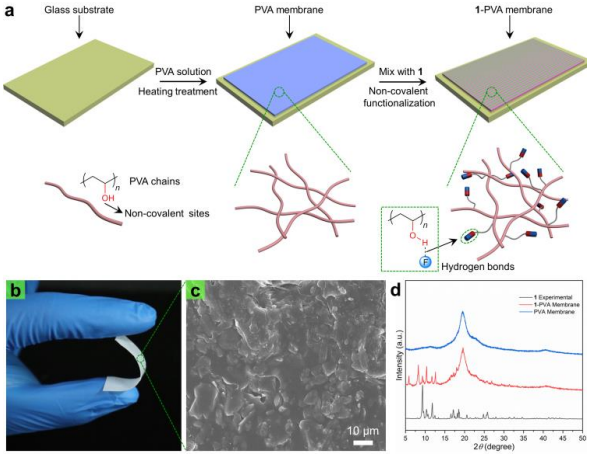

Figure 5. Stimuli-responsive behaviour of **1**-PVA membrane. a) Schematic illustration of the fabrication process of **1**-PVA photoactuator. b) Optical photo showing the flexibility of the actuator. c) Scanning electron microscopy (SEM) image of the **1**-PVA membrane surface. d) PXRD profile of **1**-PVA membrane.

In order to examine the photomechanical behavior, polymeric strips (0.5 cm × 2.0 cm) were exposed to 365 nm LED light and the photomechanical deformation was recorded. As illustrated in Figure 6a, the **1**-PVA membrane bends rapidly towards the incident light source with an angle of ~61° within 20 seconds upon exposure to 365 nm light irradiation (Movie S4). To gain further insight into the kinematics and mechanism of the photomechanical deformation, we quantified the bending angles (φ) as a function of exposure time (t) by employing a high-speed video camera (1200 frames per second) which record a series of photodeformation snapshot images (Figure 6b, Figure S25). As evident in Figure 6c, the bending angle φ increased from 0° to 58° within 12 seconds. The motion effectively stops after 20 seconds of irradiation. The bending process can be described using the following equation,

$$\varphi = k\left(1 - \exp\left(-\frac{t}{\phi}\right)\right)$$

Where k is the response time constant, t is the irradiation time, and ϕ is the actuation response time coefficient. Further details on the modelling is presented in the Note S1.

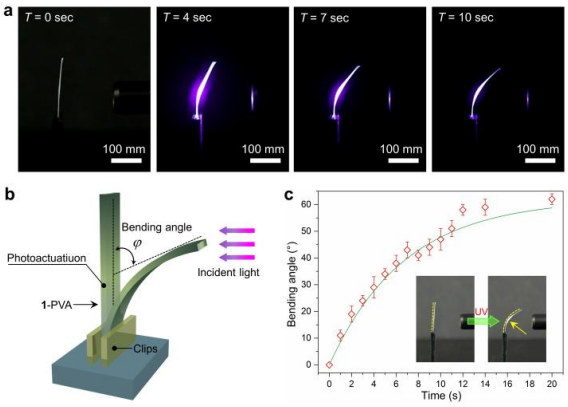

Figure 6. Mechanism of the light-driven bent actuation. a) Time-dependent photomechanical deformation of **1**-PVA upon exposure to 365 nm light. b) Schematic illustration of the experimental set-up including an indication of bending angle φ in schematic structure. c) A plot of the bending Vs exposure time with a photograph of the membrane before and after irradiation (inset).

In order to obtain more insights into the bending deformation behaviors of membrane, atomic force microscopy (AFM) was employed to probe the surfaces of the **1**-PVA and blended **1**-PVA membranes. The typical surface morphological evolution is presented in Figure S26. Following irradiation of UV light, the heterogeneous wrinkle patterns of the **1**-PVA membrane provided a contrast with the smooth surface of the pure membrane (Figure S27). The surface of the irradiated membrane has a root mean-square roughness of 201.1 nm compared to the relatively smooth pure membrane with a corresponding value of 5.1 nm. The surface roughness, indicated by the AFM images, appears to reflect the deformations resulting from the exposure to UV light.

In summary, we have succeeded in developing a photomechanical, single crystal actuator that exhibits fast response time and high sensitivity. The photomechanical behavior of this MOF-based crystal arises from the photodimerisation of olefin molecules which participate in [2+2] cycloaddition reactions. The photomechanical deformations include bending, twisting and splitting. Detailed examination of

the photomechanical deformation mechanism has been achieved using single crystal X-ray analysis and has been supported by *in situ* PXRD and ^{1}H or ^{13}C NMR spectroscopy. Of particular importance in this work is the clear demonstration of macroscopic scale photodeformation which was achieved by irradiating a composite membrane, formed by combining **1** and PVA in a thin film. We believe these results illuminate a path towards the generation of reliable photoactuator devices that are capable of delivering a substantial and reproducible mechanical response. The development of such devices has important implications for a variety of technologically useful systems including optomechanical microdevices and smart microrobotics.

Acknowledgements

This work was financially supported by the National Natural Science Foundation of China (Grants Nos. 21531006 and 21773163), and the State Key Laboratory of Organometallic Chemistry of Shanghai Institute of Organic Chemistry (Grant No. 2018kf-05), the Priority Academic Program Development of Jiangsu Higher Education Institutions and the Postgraduate Research & Practice Innovation Program of Jiangsu Province for financial support (KYCX18_2495).

Conflict of interest

The authors declare no competing financial interests.

Keywords: Photoactuators • stimulus-responsive materials • metal-organic frameworks • lattice contraction • photomechanical deformation

[1] M. Ma, L. Guo, D. G Anderson, R. Langer, *Science* **2013**, *339*, 186–189.
[2] P. M. Mendes, *Chem. Soc. Rev*. **2008**, *37*, 2512–2529.
[3] K. Xiao, G. Xie, P. Li, Q. Liu, G. L. Hou, Z. Zhang, J. Ma, Y. Tian, L. P. Wen, Jiang, *Adv. Mater*. **2014**, *26*, 6560–6565.
[4] D. Rus, M. T. Tolley, *Nature* **2015**, *521*, 467–475.
[5] a) D. Kitagawa, H. Tsujioka, F. Tong, X. Dong, C. J. Bardeen, S. Kobatake, *J. Am. Chem. Soc.* **2018**, *140*, 4208–4212; b) J. Chen, F. K. Leung, M. C. A. Stuart, T. Kajitani, T. Fukushima, E. van der Giessen, B. L. Feringa, *Nat. Chem.* **2017**, *10*, 132−138.
[6] W. A. Phillip, *Nat. Energy* **2016**, *1*, 16101.
[7] a) M. Acerce, E. K. Akdoğan, M. Chhowalla, *Nature* 2017, *549*, 370−373; b) C. Cheng, A. H. W. Ngan, *ACS Nano* **2015**, *9*, 3984–3995.
[8] M. R. Islam, X. Li, K. Smyth, M. J. Serpe, *Angew. Chem. Int. Ed.* **2013**, *52*, 10330−10333; *Angew. Chem.* **2013**, *125*, 10520−10523.
[9] Y. Hu, Z. Li, T. Lan, W. Chen, *Adv. Mater.* **2016**, *28*, 10548–10556.
[10] J. Deng, J. Li, P. Chen, X. Fang, X. Sun, Y. Jiang, W. Weng, B. Wang, H. Peng, *J. Am. Chem. Soc.* **2016**, *138*, 225−230.
[11] Q. Zhao, J. W. Dunlop, X. Qiu, F. Huang, Z. Zhang, J. Heyda, J. Dzubiella, M. Antonietti, J. Yuan, *Nat. Commun.* **2014**, *5*, 4293.
[12] X. Zhang, Z. Yu, C. Wang, D. Zarrouk, J. W. T. Seo, J. C. Cheng, A. D. Buchan, K. Takei, Y. Zhao, J. W. Ager, J. Zhang, M. Hettick, M. C. Hersam, A. P. Pisano, R. S. Fearing, A. Javey, *Nat. Commun.* **2014**, *5*, 2983.
[13] a) J. A. Lv, Y. Liu, J. Wei, E. Chen, L. Qin, Y. Yu, *Nature* **2016**, *537*, 179–184; b) D. D. Han, Y. L. Zhang, J. N. Ma, Y. Q. Liu, B. Han, H. B. Sun, *Adv. Mater.* **2016**, *28*, 8328–8343.
[14] a) T. Ikeda, J. I. Mamiya, Y. Yu, *Angew. Chem. Int. Ed.* **2007**, *46*, 506–528; *Angew. Chem.* **2007**, *119*, 512–535; b) S. Kobatake, S. Takami, H. Muto, T. Ishikawa, M. Irie, *Nature* **2007**, *446*, 778−781.
[15] a) D. Kitagawa, H. Nishi, S. Kobatake, *Angew. Chem. Int. Ed.* **2013**, *52*, 9320−9322; *Angew. Chem.* **2013**, *125*, 9490–9492; b) R. Medishetty, A. Husain, Z. Bai, T. Runcevski, R. E. Dinnebier, P. Naumov, J. J. Vittal, *Angew. Chem. Int. Ed.* **2014**, *53*, 5907−5911; *Angew. Chem.* **2014**, *126*, 6017−6021; c) R. Medishetty, S. C. Sahoo, C. E. Mulijanto, P. Naumov, J. J. Vittal, *Chem. Mater.* **2015**, *27*, 1821−1829.
[16] F. Tong, W. Xu, M. Al-Haidar, D. Kitagawa, R. O. Al-Kaysi, C. J. Bardeen, *Angew. Chem. Int. Ed.* **2018**, *57*, 7080–7084; *Angew. Chem.* **2018**, *130*, 7198–7202.
[17] K. Kumar, C. Knie, D. Bleger, M. A. Peletier, H. Friedrich, S. Hecht, D. J. Broer, M. G. Debije, A. P. H. J. Schenning, *Nat. Commun.* **2016**, *7*, 11975.
[18] a) E. Uchida, R. Azumi, Y. Norikane, *Nat. Commun.* **2015**, *6*, 7310; b) Q. Li, G. Fuks, E. Moulin, M. Maaloum, M. Rawiso, I. Kulic, J. T. Foy, N. Giuseppone, *Nat. Nanotechnol.* **2015**, *10*, 161−165; c) Q. Yu, X. Yang, Y. Chen, K. Yu, J. Gao, Z. Liu, P. Cheng, Z. Zhang, B. Aguila, S. Ma, *Angew. Chem., Int. Ed.* **2018**, *57*, 10192–10196; *Angew. Chem.* **2018**, *130*, 10349–10353; d) P. Gupta, D. P. Karothu, E. Ahmed, P. Naumov, N. K. Nath, *Angew. Chem., Int. Ed.* **2018**, *57*, 8498–8502; *Angew. Chem.* **2018**, *130*, 8634–8638; e) S. C. Sahoo, N. K. Nath, L. Zhang, M. H. Semreen, T. H. Al-Tel, P. Naumov, *RSC Adv.* **2014**, *4*, 7640–7647.
[19] a) Y. Gu E. A. Alt, H. Wang, X. Li, A. P. Willard, J. A. Johnson, *Nature* **2018**, *560*, 65−69; b) Q. Zhao, J. Heyda, J. Dzubiella, K. Täuber, J. W. Dunlop, J. Yuan, *Adv. Mater.* **2015**, *27*, 2913–2917; c) P. Naumov, S. Chizhik, M. K. Panda, N. K. Nath, E. Boldyreva, *Chem. Rev.* **2015**, *115*, 12440–12490.
[20] W. Jiang, D. Niu, H. Liu, C. Wang, T. Zhao, L. Yin, Y. Shi, B. Chen, Y. Ding, B. Lu, *Adv. Funct. Mater.* **2014**, *24*, 7598–7604.
[21] a) T. Lan, W. Chen, *Angew. Chem. Int. Ed.* **2013**, *52*, 6496–6500; *Angew. Chem.* **2013**, *125*, 6624–6628; b) H. H. Cheng, J. Liu, Y. Zhao, C. G. Hu, Z. P. Zhang, N. Chen, L. Jiang, L. T. Qu, *Angew. Chem. Int. Ed.* **2013**, *52*, 10482–10486; *Angew. Chem.* **2013**, *125*, 10676–10680.
[22] a) H. C. Zhou, J. R. Long, O. M. Yaghi, *Chem. Rev.* **2012**, *112*, 673–674; b) H. Furukawa, K. E. Cordova, M. O'Keeffe, O. M. Yaghi, *Science* **2013**, *341*, 1230444.
[23] a) Z. Hu, B. J. Deibert, J. Li, *Chem. Soc. Rev.* **2014**, *43*, 5815–5840; b) L. E. Kreno, K. Leong, O. K. Farha, M. R. P. Allendorf, Van Duyne, J. T. Hupp, *Chem. Rev.* **2011**, *112*, 1105–1125.
[24] W. Lin, W. J. Rieter, K. M. Taylor, *Angew. Chem. Int. Ed.* **2009**, *48*, 650–658; *Angew. Chem.* **2009**, *121*, 660–668.
[25] J. Liu, L. Chen, H. Cui, J. Zhang, L. Zhang, C. Y. Su, *Chem. Soc. Rev.* **2014**, *43*, 6011–6061.
[26] a) C. Y. Lee, O. K. Farha, B. J. Hong, A. A. Sarjeant, S. T. Nguyen, J. T. Hupp, *J. Am. Chem. Soc.* **2011**, *133*, 15858–15861; b) T. Zhang, W. Lin, *Chem. Soc. Rev.* **2014**, *43*, 5982–5993.
[27] a) N. K. Nath, T. Runcevski, C. Y. Lai, M. Chiesa, R. E. Dinnebier, P. Naumov, *J. Am. Chem. Soc.* **2015**, *137*, 13866−13875; b) S. Y. Yang, X. L. Deng, R. F. Jin, P. Naumov, M. K. Panda, R. B. Huang, L. S. Zheng, B. K. Teo, *J. Am. Chem. Soc.* **2013**, *136*, 558−561.
[28] G. M. J. Schmidt, *Pure Appl. Chem.* **1971**, *27*, 647–678.
[29] D. Kitagawa, K. Kawasaki, R. Tanaka, S. Kobatake, *Chem. Mater.* **2017**, *29*, 7524−7532.
[30] Z. Li, X. Zhang, S. Wang, Y. Yang, B. Qin, K. Wang, T. Xie, Y. Wei, Y. Ji, *Chem. Sci.* **2016**, *7*, 4741−4747.
[31] H. Wang, P. Chen, Z. Wu, J. Zhao, J. Sun, R. Lu, *Angew. Chem. Int. Ed.* **2017**, *56*, 9463–9467; *Angew. Chem.* **2017**, *129*, 9591–9595.
[32] M. K. Panda, S. Ghosh, N. Yasuda, T. Moriwaki, G. D. Mukherjee, C. M. Reddy, P. Naumov, *Nat. Chem.* **2015**, *7*, 65−72.
[33] Y. Yue, Y. Norikane, R. Azumi, E. Koyama, *Nat. Commun.* **2018**, *9*, 3234.
[34] a) Y. Li, L. Liang, C. Liu, Y. Li, W. Xing, J. Sun, *Adv. Mater.* **2018**, *30*, 1707146; b) B. R. Tiwari, Md. T. Noori, M. M. Ghangrekar, *Mater. Chem, Phys*. **2016**, *182*, 86-93.

Entry for the Table of Contents (Please choose one layout)

COMMUNICATION

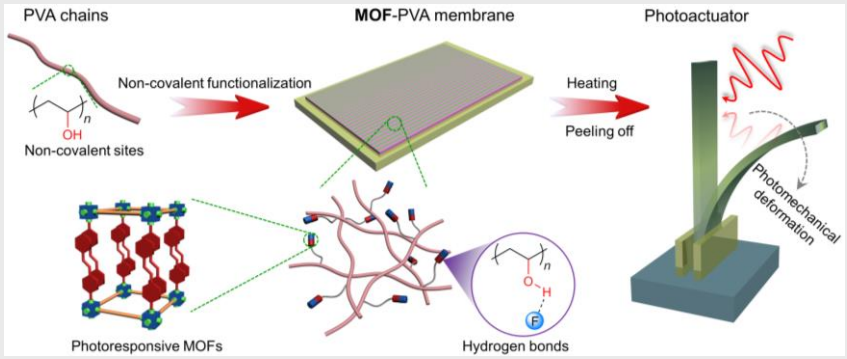

*Yi-Xiang Shi, Wen-Hua Zhang, Brendan F. Abrahams, Pierre Braunstein, and Jian-Ping Lang,**

Page No. – Page No.

Fabrication of New Photoactuators: Macroscopic Photomechanical Responses of Metal-Organic Frameworks to Irradiation by UV Light

A self-assembly strategy for the fabrication of a hierarchical photoactuator system in which a photoresponsive moiety is incorporated into a MOF crystal. Additionally, we have successfully fabricated a photoactuation system which involves a MOF-PVA composite membrane which exhibits a macroscopic response upon exposure to UV light irradiation.